

Validation of the SPACE Code through Simulated Accident Scenarios in SMART-ITL: A Focus on Pressurizer Safety Valve Break and Safety Injection Line Break Concurrent with TLOSHR

Sultan Al-Faifi ^{a*}, Eslam Bali ^a, Kyung Doo Kim^b

^aKing Abdullah City for Atomic and Renewable Energy, Riyadh 12244, Saudi Arabia

^bKorea Atomic Energy Research Institute, 989-111 Daedeokdaero, Yuseong, Daejeon, 305-353, Korea

*Corresponding author: s.faifi@energy.gov.sa

Abstract - Nuclear system analysis codes must demonstrate their capabilities in order to be licensed for usage in the design and safety analysis of nuclear power plant. The Safety and Performance Analysis Code (SPACE) has been developed and approved to be used for licensing applications of Pressurized Water Reactors (PWRs). However, since new innovative designs such as SMART100, a 100 MWe system-integrated modular advanced reactor, incorporate inherent and passive safety features that are not used in conventional loop-type reactors, special models should be developed and validated to reflect the characteristics of the SMART-100 and obtain reliable predictions. A thermal-hydraulic integral effect test facility, SMART-ITL, was constructed to evaluate the system performance of SMART-100 and investigate the thermal-hydraulic phenomena that occur in the reactor systems and components under normal, abnormal, and emergency conditions. The experimental data also serves to validate the related thermal-hydraulic models of the safety analysis codes. This study presents a validation of the SPACE code, using the SMART-ITL facility, to evaluate its applicability for analyzing thermal hydraulics in integral reactors. Simulations were performed for two experimental test scenarios: pressurizer safety valve break and safety injection line break concurrent with total loss of secondary heat removal (TLOSHR). The validation results indicate that the SPACE code accurately predicted key thermal hydraulic behaviors, such as primary and secondary system pressures and temperatures. However, a slight underestimation of the RPV's water level was observed, attributed mainly to the overestimation of the accumulated break flow due to inaccuracies in the two-phase critical flow models.

Keywords: SPACE, SMART-100, SMART-ITL, SBLOCA, System Analysis Codes, SMRs

I. Introduction

Demonstrations of the capabilities of nuclear system analysis codes are required to obtain a license for their use in various applications in nuclear power plants. They can be used in the design and safety evaluation of nuclear power plants to help assess the performance and safety margins of reactor components under various operational and accident scenarios, such as Design Basis Accidents (DBAs) and Design Extension Conditions (DECs). DBAs consider situations where something goes wrong but the safety systems function as intended while DECs consider more extreme scenarios, including the potential failure of one or more safety systems.

The Safety and Performance Analysis Code (SPACE) has been developed and approved to be used for licensing applications of Pressurized Water Reactors (PWRs) in 2017. However, since new innovative designs such as the SMART-100, a 100 MWe system-integrated modular advanced reactor, incorporate inherent and passive safety design features that are not used in conventional loop-type reactors, special models should be developed and validated to reflect the characteristics of the SMART-100 and obtain reliable predictions.

In general, the prediction results of system analysis codes may be inconsistent with the experimental results due to various uncertainties in numerical schemes, empirical correlations, and user errors [1]. To enhance the reliability of the simulation results, validation work for many kinds of separate effect tests and integral effect tests is required. Therefore, this paper's objective lies in the assessment of the SPACE code's accuracy, accomplished by validating two accident scenarios, both representing SBLOCA (small break loss of coolant accidents), but with one reflecting a DBA and the other representing a DEC scenario. The first accident scenario is initiated by a break in the Pressurized Safety Valve (PSV), with all safety systems operating as intended, while the subsequent scenario arises from a rupture in the SMART-ITL's Safety Injection Line (SIL), concurrent with a Total Loss of Secondary Heat Removal (TLOSHR).

The paper first introduces the SMART-ITL facility and SPACE code nodalization, followed by an in-depth representation of the accident scenarios. Finally, it discusses the comparison of the simulated results and the experimental findings for each scenario.

II. SBLOCA of PSV

II. A. Overview of SPACE

The SPACE code, a safety and performance analysis tool, is commonly employed in the design and analysis of Pressurized Water Reactors (PWRs). This safety analysis tool was officially authorized by the Nuclear Safety and Security Commission (NSSC) in 2017, allowing it to be used in the licensing processes of Korean Pressurized Water Reactors (PWRs). The SPACE code is capable of high-fidelity simulations of accidents such as the loss of coolant, the main steam line break, the main feed water line break, and the steam generator tube rupture that are required in the safety analyses of PWRs. The code incorporates advanced physical modeling of two-phase flows, with a primary emphasis on two-fluid, three-field models, which consist of gas, continuous liquid, and droplet fields. [2]

II. B. Overview of SMART-ITL

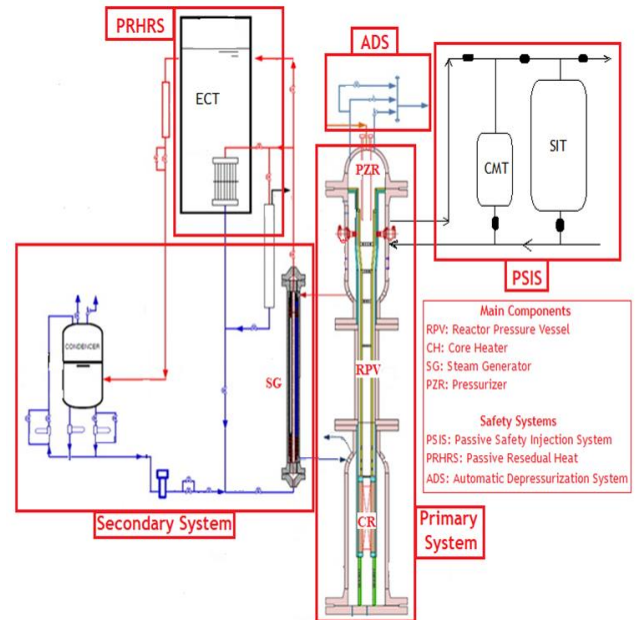


Fig. 1. Simplified schematic diagram of SMART-ITL facility

The SMART-ITL is a thermal-hydraulic integral effect test facility for SMART. It is designed based on the volume scaling methodology, in which the height of the individual components is conserved and the flow area and volume are scaled down to 1/49. It has the same integral features as SMART except for the externally installed Steam Generators (SGs). The main objectives of the

SMART-ITL are to investigate and understand the integral behavior and the thermal hydraulic phenomena occurring in the reactor systems and components during normal, abnormal, and emergency conditions [3&4]. The integral-effect test data are also used to validate the related thermal-hydraulic models of the safety analysis codes, which can be used for a performance and accident analysis of the SMART design [5]. A simplified schematic diagram of the SMART-ITL facility is shown in Fig 1.

The SMART-ITL consists of a primary system, a secondary system, safety-related systems, a break simulating system (BSS), a break measuring system (BMS), and auxiliary systems. The primary system is composed of the reactor pressure vessel (RPV), SGs, and primary connecting piping between the Reactor Pressure Vessel (RPV) and SGs. The secondary system of the SMART-ITL is simplified to be of the circulating loop type and is composed of a condenser, feed water and steam lines, and related piping and valves. The safety-related systems include four trains of the Passive Residual Heat Removal System (PRHRS), four trains of the Passive Safety Injection Systems (PSIS), and two trains of the Automatic Depressurization Systems (ADS). The PRHRS was designed to remove the decay heat by natural circulation in an emergency situation, while the PSIS was designed to inject borated water into the RCS by gravity head to prevent core uncover in LOCA scenarios. The ADS helps to rapidly depressurize the RCS to activate Safety Injection Tanks (SIT) earlier during the LOCA accident.

II. C. Overview of PSV LOCA

The PSV LOCA is caused by a break in the pressurizer safety valve connecting to the RCS pressure boundary. Upon the occurrence of this break, reactor coolant is discharged and the pressurizer (PZR) pressure decreases. Once the PZR pressure reaches the low PZR pressure (LPP) setpoint (10.26 MPa), the reactor trip signal is generated, and the heater power follows a decay curve (1.2×ANS-73 residual heat curve required on 10CFR50 Appendix K) [3]. Coinciding with this event is the Loss of Offsite Power (LOOP), assumed to occur simultaneously with a turbine trip. This results in a simultaneous power cut to the Reactor Coolant Pumps (RCPs) and the feed water pumps. In response to this sequence of events, the PRHRAS is generated due to the low feed water flow rate, leading to the activation of the PRHRS. With the actuation of PRHRS, the residual heat of the core is removed which in turn continuously

decreases the RCS pressure. Upon reaching the LPP signal, the Core Makeup Tank Actuation Signal (CMTAS) is generated. This action triggers the injection of the water contained in the Core Makeup Tank (CMT) into the Reactor Pressure Vessel (RPV) by gravitational force to compensate for the discharging of the RCS and prevent the reactor core from uncovering. When the PZR pressure decreases further to the SIT actuation signal (SITAS) set point, the cold water in the SIT is also injected into the RPV to maintain the RCS inventory. Throughout this transient, only saturated steam is released through the break. Hence, the injection of the water from the CMTs and SITs into the RPV recovers the water level. Consequently, coolant and fuel temperatures demonstrate a consistent decrease. The sequence of events for the SB-PSIS-F301 test is detailed in Table I.

Table I Sequence of events for SB-PSIS-F301 test [3]

Sequence of Events	Set point / Trip signal	Time (s)
Steady-state	-	-744
Accident start	Break in PSV	0
Reactor trip setpoint reached	LPP=10.26 MPa	204
Reactor trip signal generation	LPP+1.1 s	205
Turbine trip		
RCP coastdown start		
Feed water stop		
CMTAS generation		
Control rod insertion	Decay heat table	206
CMT injection	LPP+2.2 s	206
PRHRS valve open	LPP+10.2 s	214
FIV/MSIV close	LPP+10.2	215
SITAS generation	LLPP=2 MPa	4,127
SIT injection	SITAS+1.1 s	4,131
ADS #1 open	CMT level= 35%	24,093
Experiment termination	-	261,326

II. D. Nodalization of the SMART-ITL

A simplified nodalization of the SPACE code for SMART-ITL is illustrated in Fig. 2. Systems like the RCS, secondary systems, Safety Injection Tanks (SITs), Core Makeup Tanks (CMTs), and the PRHRS are modeled with cells and faces.

The RCS is comprised of a heater to simulate the reactor core, upper plenum, RCPs, SGs primary side, downcomer, core bottom region, and the PZR. In order to simulate the heat loss through the reactor pressure vessel,

heat structures with proper geometries, material properties, and outer boundary conditions are attached to the outer cells.

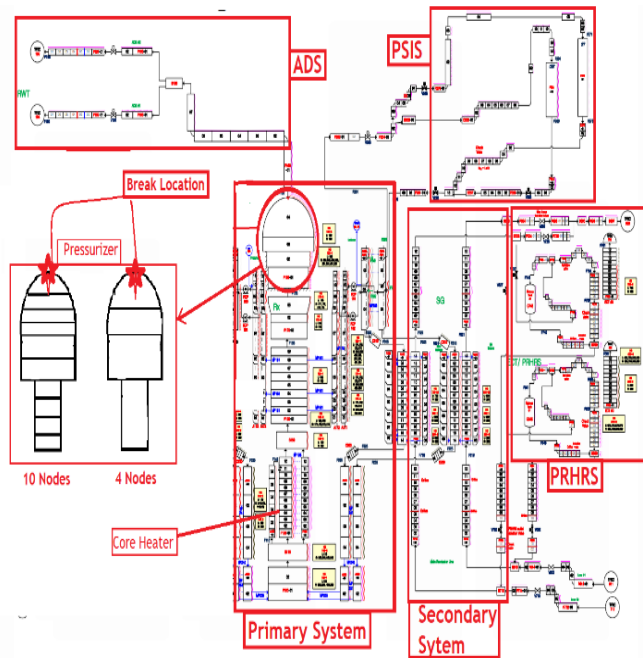


Fig. 2. Simplified nodalization for single train of SMART-ITL facility

II.E. Steady-State Condition

The steady-state calculation is performed to verify the input nodalization of the SPACE code for the SBPSIS-F301 test. For the steady-state calculation, averaged data of the thermal hydraulic parameters of the RCS, secondary system, PSIS, and PRHRS are used. The major thermal hydraulic parameters of the SB-PSIS-F301 test at steady-state are listed in Table II. Throughout the steady-state phase, the RCS flow rate was maintained at 10.46 kg/s. The SG inlet and outlet temperatures were measured as 594.3 K (321.2 °C) and 571.9 K (298.8 °C), respectively. In the secondary system, subcooled feed water is supplied to the SG to extract the thermal energy of the primary system, resulting in the production of superheated steam. The feed water flow rate and the steam pressure were measured at 0.774 kg/s and 5.63 MPa, respectively.

The steady-state calculation of SPACE was performed for 3000 seconds, and the results are summarized in Table II. It was confirmed that the steady-state results of the SPACE calculation for the major parameters were in very good agreement with the experimental values. Therefore, a transient simulation was subsequently initiated based on the results of this steady state analysis. The Henry-Fausky critical flow model is used with discharge coefficients of 0.75 and 0.4 for single-phase and two-phase flow,

respectively.

Table II Steady-state calculation results for SB-PSIS-F301 test

Parameter	EXP	SPACE	Error (%)
Power (MW)	1.693	1.693	BC
Core Inlet Temp (K)	569.6	569.2	-0.07
Core Outlet Temp (K)	594.2	594.6	0.07
SG Primary Inlet Temp (K)	594.3	594.6	0.05
SG Primary Outlet Temp (K)	571.9	571.2	-0.12
PZR pressure (MPa)	15	15	BC
PZR level (m)	3.17	3.16	-0.32
RCS flow rate (kg/s)	10.46	10.46	BC
SG Secondary Inlet Temp (K)	503.1	503.1	BC
SG Secondary Outlet Temp (K)	587.9	594.5	1.12
Feed Water Flow rate (kg/s)	0.774	0.774	BC
Feed Water Pressure (MPa)	5.72	5.72	BC
Mean Steam Pressure (Mpa)	5.63	5.632	0.04

II.F. Results and Discussion

After obtaining a good agreement between the code calculation and the experimental results, the steady state results were used as initial conditions for the transient calculation, and the results of the main parameters are shown as follows:

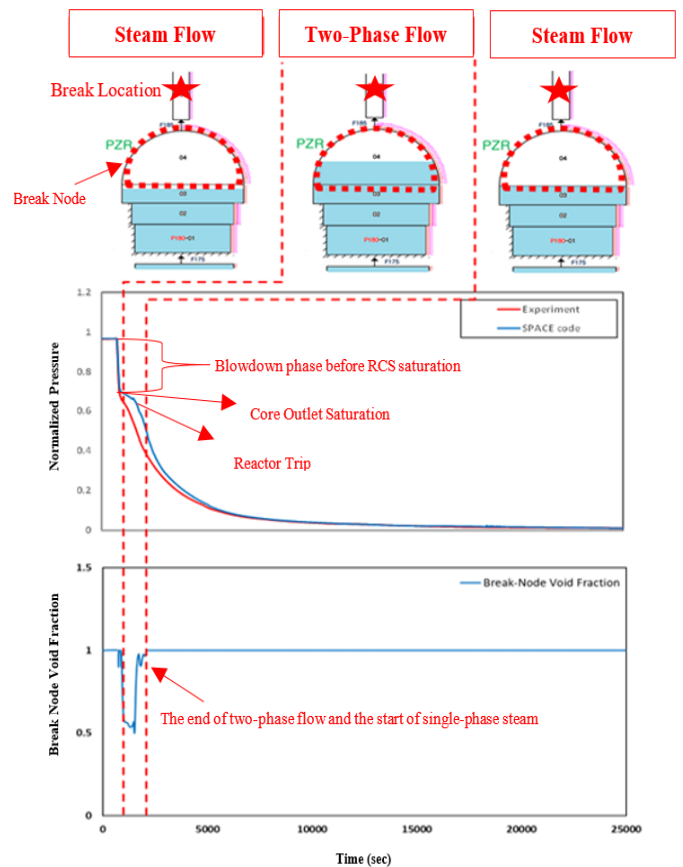


Fig. 3. Comparison of Pressurizer pressure

Fig. 3 shows the behavior of the PZR pressure. When a PSV break occurs, the PZR pressure drops rapidly during the blowdown phase until it reaches the saturation pressure of the core outlet temperature. Then, the depressurization rate decreased owing to the high steam generation in the core. After a short period, the PZR pressure reached the LPP set point of 10.26 MPa, and the reactor trip signal by the LPP was generated. Consequently, the core power started to decrease according to the simulated decay heat of the experiment. Moreover, the simultaneous assumption of LOOP led to the coastdown of the RCPs, and the flow pattern was changed from forced circulation to natural circulation. The system pressure decreased continuously until the end of the scenario.

The SPACE code predicts the overall depressurization behavior comparatively well but slightly underpredicts the depressurization rate at the end of the blowdown phase, which resulted in a delay of the reactor trip. The overprediction was clearly a result of the existence of two-phase flow in the break node after the swelling of the RCS. Therefore, while only a discharge of single-phase steam flow was observed in the experiment, the SPACE code predicted two-phase flow at the onset of the accident. This error can have an impact not only on the depressurization rate but also on the break flow rate. That is because the release of two-phase flow instead of single-phase steam flow leads to a lower depressurization rate and a higher break flow rate. Those effects can be shown in Fig. 3 and Fig. 4, respectively.

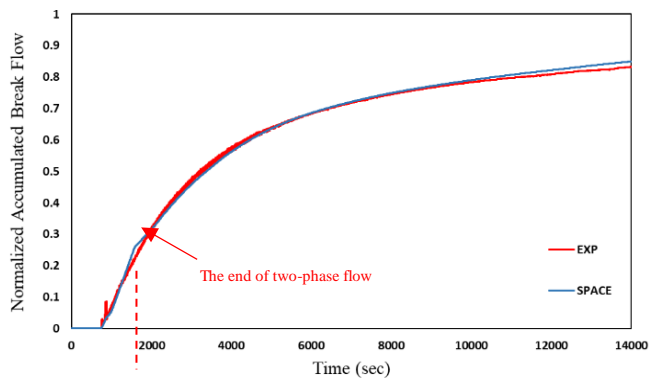


Fig. 3. Comparison of accumulated break flow

Fig. 4 shows a comparison of accumulated break flow rate between SPACE code and the experiment. The SPACE code shows excellent prediction for the selected critical flow model and discharge coefficients.

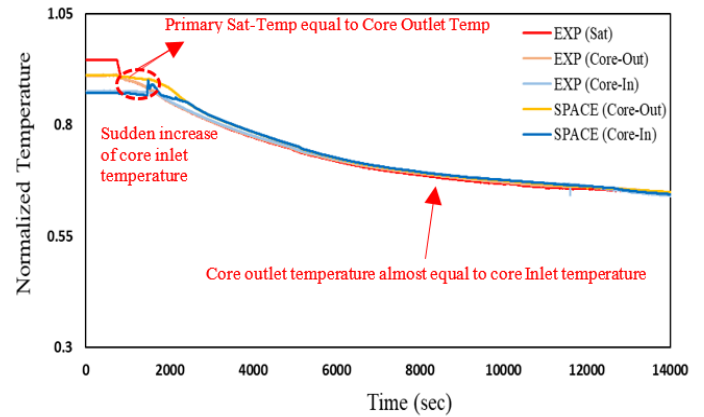


Fig. 4. Comparison of core inlet and outlet temperatures

Fig. 5 shows the fluid temperatures at the core inlet and outlet. In the experiment, the fluid temperatures decreased with the saturation temperature corresponding to the system pressure. After the reactor trip, a sudden increase in the calculated core inlet temperature was observed due to insufficient heat removal from the decay heat. As the PRHRS actuated and the natural circulation established in the secondary side, the decay heat was removed continuously, and the fluid temperature at the core inlet and outlet decreased gradually until the end of the accident. The SPACE code correctly predicts the overall fluid temperatures while maintaining saturation condition.

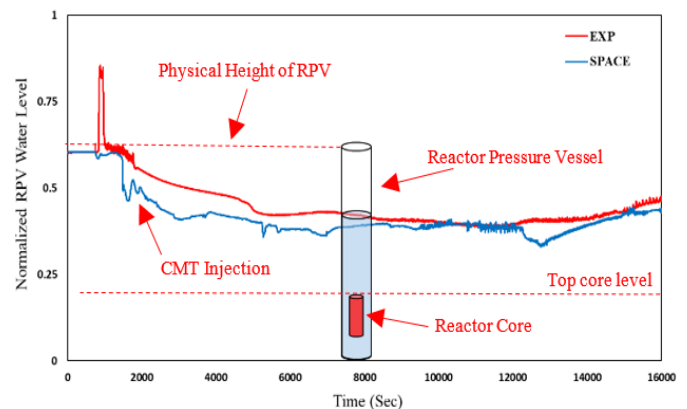


Fig. 5. Comparison of RPV collapsed water level

Fig. 6 shows the collapsed water level in the reactor pressure vessel. In the test, the water level rose suddenly after the break and then rapidly dropped. After that, the water level gradually decreased until it was stabilized by the actuation of the CMT. However, during the sudden rise of the water level, which was measured based on the pressure difference, the measured value exceeded the actual height of the RPV. This error was a result of the improper mounting position of the instrument, which was installed in the break line of the PSV. Because of the

improper position, the sudden change in the dynamic pressure after the break resulted in a sudden reduction in the static pressure at the same position, resulting in a higher pressure difference and a collapsed water level. The minimum collapsed water level was 6.2 m higher than the core top elevation. The SPACE code reasonably predicts the collapsed water level, with a slight underprediction at the start of the transient due to the early discharge of two-phase flow.

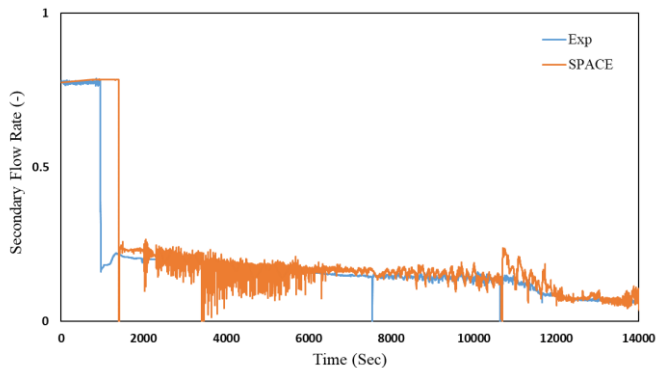


Fig. 6. Comparison of secondary flow rate

Fig. 7 represents the total flow rate in the secondary system. It is clearly shown that the normal feed water flow rate was maintained before the actuation of PRHRS. Following a reactor shutdown, PRHRS operation started, and a stable natural circulation flow rate was established after a few seconds. Subsequently, a gradual decrease of the natural circulation with a constant rate was shown owing to the decay of heat on the primary side. As shown in the graph, there was a lag in the PRHRS activation in the system due to the delay of the reactor trip signal. However, the SPACE code properly predicts the overall natural circulation flow rate in the secondary system.

III. SBLOCA of SIL concurrent with TLOSHR (DEC Scenario)

III.A. Overview of SIL LOCA

The SIL LOCA is caused by a break in the safety injection line connecting to the RCS pressure boundary. As the break occurs, reactor coolant is discharged through the break area, and the Pressurizer (PZR) pressure decreases. When the PZR pressure reaches the low PZR pressure (LPP) reactor trip setpoint (10.26 MPa), the reactor trip signal is generated, and the heater power follows a decay curve ($1.2 \times \text{ANS-73}$ residual heat curve required on 10CFR50 Appendix K) [3]. The loss of offsite power (LOOP) is considered a coincidence, and the power to the RCPs and the feed water pumps is lost simultaneously with the turbine trip. Consequently, the

PRHRAS is generated by the low feed water flow rate, but the PRHRS fails to operate. The RCS pressure decreases continuously due to the loss of coolant mass and energy through the break flow. As the CMT actuation signal (CMTAS) is generated by the LPP signal, the CMT isolation valves are opened. Consequently, the water in the CMT is injected into the RPV by the gravitational force after the emptying of the pressure balance line in the PSIS.

At the onset of the transient, subcooled water is released through the break. As the PZR pressure decreases to saturation pressure and the water level in the RPV decreases to the break location, the phase of the break flow changes to a two-phase mixture, followed by steam. With the subsequent injection of the water from the CMT into the RPV, the water level inside the RPV is recovered. Throughout the transient, the core is covered with water, and thus the coolant temperatures as well as the fuel temperatures are monotonically decreased. The sequence of events for the SB-PSIS-F101 test is illustrated in Table III.

Table III Sequence of events for SB-PSIS-F301 test [3]

Sequence of Events	Set point / Trip signal	Time (s)
Steady-state	-	-744
Accident start	Break in SIL	0
Reactor trip setpoint reached	LPP=10.26 MPa	630
Reactor trip signal generation	LPP+1.1 s	631
Turbine trip		
RCP coastdown start		
Feed water stop		
CMTAS generation		
Control rod insertion	Decay heat table	632
CMT injection	LPP+2.2 s	632
Generation of PRHRSAS (PRHRS failed to operate)	LPP+5.2 s	632
FIV/MSIV close	LPP+10.2	641
Experiment termination	-	42708

III.B. Nodalization of the SMART-ITL

The nodalization of this accident scenario is exactly similar to the previous one but the PRHRS, ADS, and SITs were not actuated.

III.C. Steady-State Condition

The steady-state calculation is performed to verify the input nodalization of the SPACE code for the SBPSIS-F101 test. For the steady-state calculation, the averaged test results of the thermal hydraulic parameters of the RCS, secondary system, PSIS, and PRHRS are used. The major thermal hydraulics parameters of the SB-PSIS-F101 test at steady-state are listed in Table III. During the

steady state, the measured RCS flow rate was maintained at 10.397 kg/s, while the calculated flow rate is 11.52kg/s. This is because the calculated flow rate is adjusted in order to match the temperature difference between the core inlet and outlet with the experimental measurements. The SG inlet and outlet temperatures are 594.3 K (321.2 °C) and 571.9 K (298.8 °C), respectively. In the secondary system, the subcooled feed water is supplied to the SG to remove the heat from the primary system and become superheated steam. The feed water flow rate is 0.778 kg/s, and the steam pressure is 5.63 MPa. Table IV shows a comparison between SMART-ITL major thermal hydraulics parameters with the calculation results of SPACE. The steady-state results of the SPACE calculation for the selected parameters were in a very good agreement with experimental values.

Table IV Steady-state calculation results for SB-PSIS-F101 test

Parameter	EXP	SPACE	Error (%)
Power (MW)	1.6723	1.6723	BC
Core Inlet Temp (K)	568.7	569.4	0.12
Core Outlet Temp (K)	594.1	594.7	0.1
SG Primary Inlet Temp (K)	594.3	594.5	0.03
SG Primary Outlet Temp (K)	571.9	571.7	-0.04
PZR pressure (MPa)	15	15	BC
PZR level (m)	2.972	2.973	-0.32
RCS flow rate (kg/s)	10.397	11.52	Adjusted
SG Secondary Inlet Temp (K)	503.15	503.15	BC
SG Secondary Outlet Temp (K)	575.45	575.45	-5.3
Feed Water Flow rate (kg/s)	0.778	0.774	Adjusted
Feed Water Pressure (MPa)	5.71	5.71	BC
Mean Steam Pressure (Mpa)	5.63	5.632	0.04

III.D. Results and Discussion

After alignment between the code calculation and the experiment, the steady-state conditions are used as initial conditions for the transient calculation. However, before evaluating the results of the main parameters, a sensitivity analysis to select proper critical flow models and discharge coefficients should be performed as follows:

Since the behavior of the primary and secondary loops heavily depends on the accumulated break flow, it is crucial to perform a sensitivity analysis to find the effect of different critical flow models and discharge coefficients on the calculation results of the SPACE code and to select the optimal settings for the simulation. As shown in Fig. 8, at equivalent discharge coefficients, the calculation results of the Henry-Fauske critical flow model resulted in higher accumulated break flows and thus higher depressurization rates compared to the Ransom-Trapp model. Furthermore, a best-fitting curve to the accumulated break flow resulted in a long delay of

the reactor trip owing to the low depressurization rate. On the other hand, a best-fit curve to the depressurization rate resulted in an overestimation of the accumulated break flow, which can lead to a core uncover. Therefore, by taking into consideration the accumulated break flow and the depressurization rate, the Ransom-Trapp model with default discharge coefficients was used.

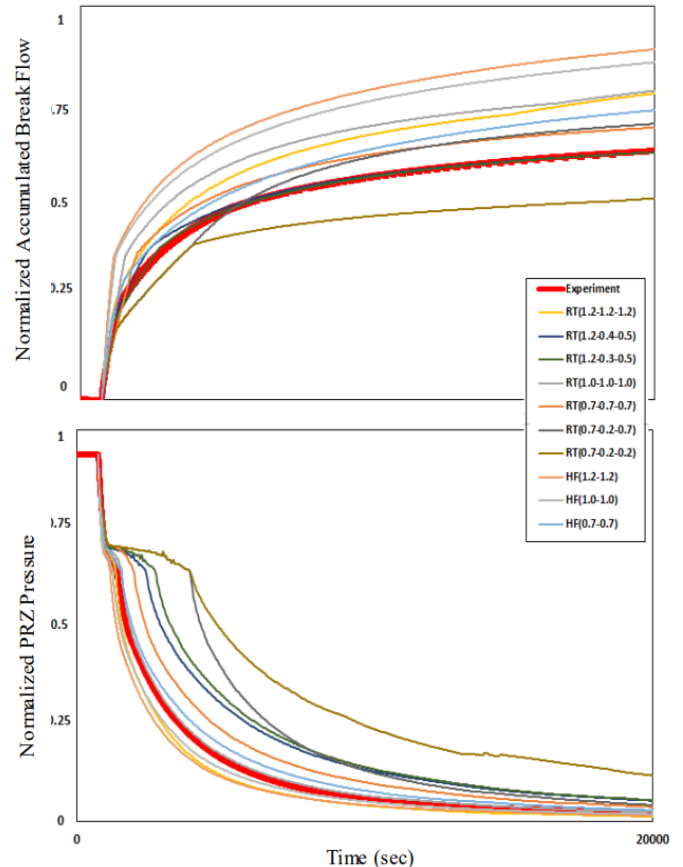


Fig. 8. Sensitivity analysis of critical flow models and discharge coefficients

Fig. 9 shows the pressure behavior of the primary system. When the SIL break occurred, the PZR pressure decreased rapidly during the blowdown phase. As soon as the PZR pressure matched the saturation pressure of the core outlet temperature, the rate of depressurization reduced due to high evaporation rates in the primary system. The depressurization rates decreased due to the high evaporation rates in the primary system. After a short period, the PZR pressure reached the LPP setpoint of 10.26 MPa, and the reactor trip signal by the LPP was generated. Consequently, the core power started to decrease according to the simulated decay heat of the experiment. With the simultaneous assumption of LOOP, the RCP started to coastdown and the forced flow circulation was terminated. After the reactor trip, the system pressure decreased continuously until the end of

the scenario. The SPACE code predicts the depressurization behavior comparatively well.

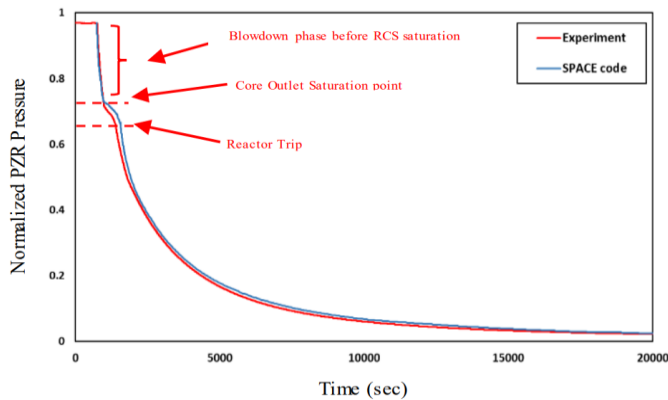


Fig. 9. Comparison of pressurizer pressure for SBLOCA

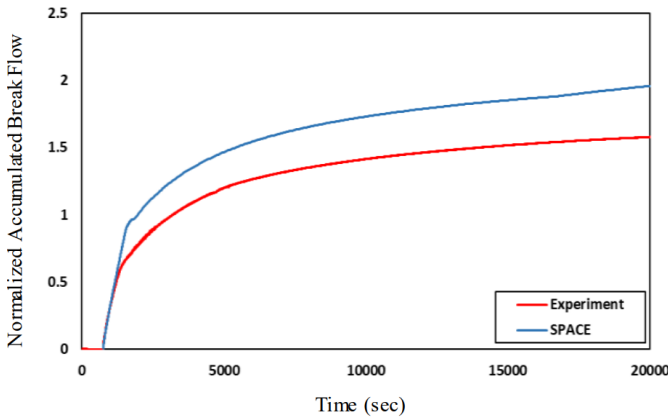


Fig. 10. Comparison of accumulated break flow

Fig. 10 shows a comparison of the accumulated break flow rate between the SPACE code and the experiment. The SPACE code shows a reasonable prediction for both single-phase subcooled liquid and steam. The overprediction of the code occurs in the two-phase time period, which can be clearly seen in Fig. 11.

According to the evaluation of the accumulated break flow, the subcooled flow and the single-phase steam flow are well predicted by the SPACE code, as shown in Fig. 11. However, the code overpredicts the break flow rates during the two-phase flow period. This is mainly due to the inaccuracy of the critical flow models during the two-phase flow period. Therefore, the users of the code should always take into consideration the existence of the two-phase in the break node and their significant impact on the depressurization rate and the break flow rate.

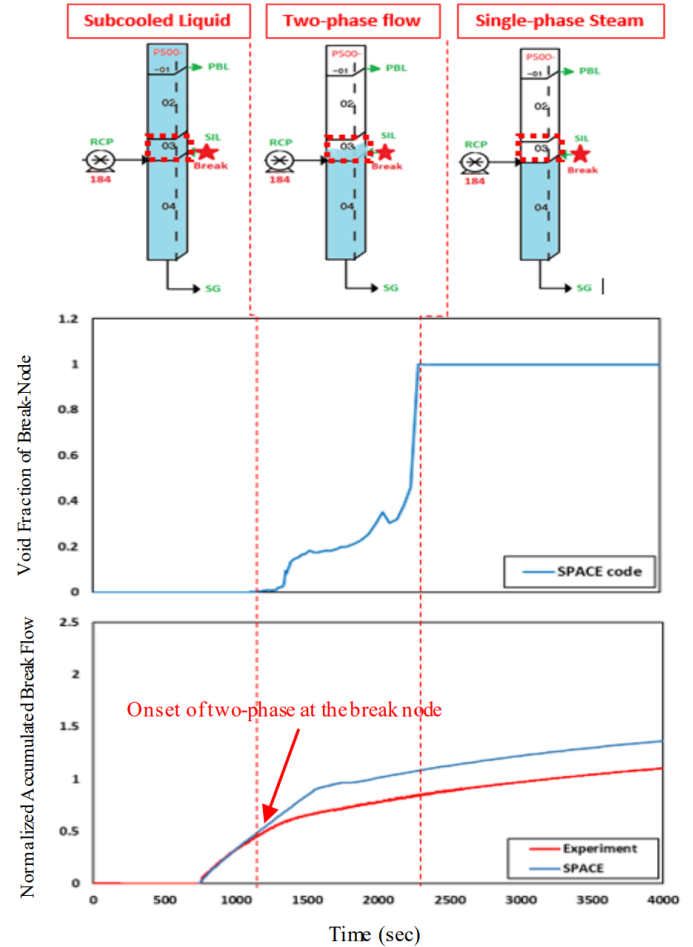


Fig. 11. Reason of the overestimation in the accumulated break flow

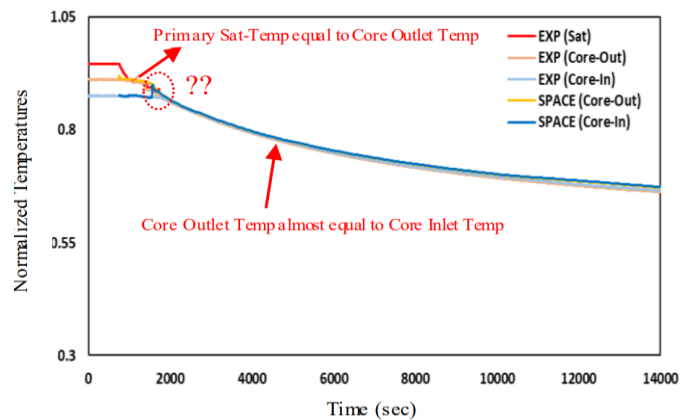


Fig. 12. Comparison of core inlet and outlet temperatures

Fig. 12 shows the fluid temperatures at the core inlet and outlet. In the experiment, the fluid temperatures decreased with the saturation temperature corresponding to the system pressure. After the reactor trip, a sudden increase in the calculated core inlet temperature was observed due to insufficient heat removal from reactor core. The decay heat was removed continuously through

the break, and thus the fluid temperature at the core inlet and outlet decreased gradually until the end of the accident. The SPACE code properly predicts the overall fluid temperatures while maintaining saturation.

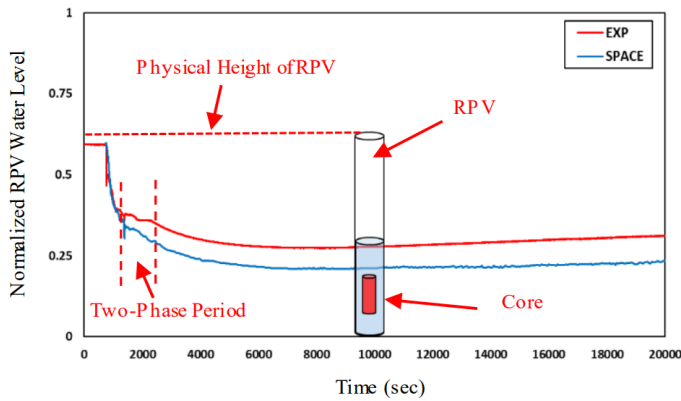


Fig. 13. Comparison of RPV collapsed water level

Fig. 13 shows the collapsed water level in the reactor pressure vessel. In the test, the water level decreased after the break and stabilized after the actuation of the CMT. The minimum collapsed water level was higher than the core top elevation. The SPACE code underpredicts the collapsed water level owing to the overprediction of the break flow rate during the existence of the two-phase flow in the break node.

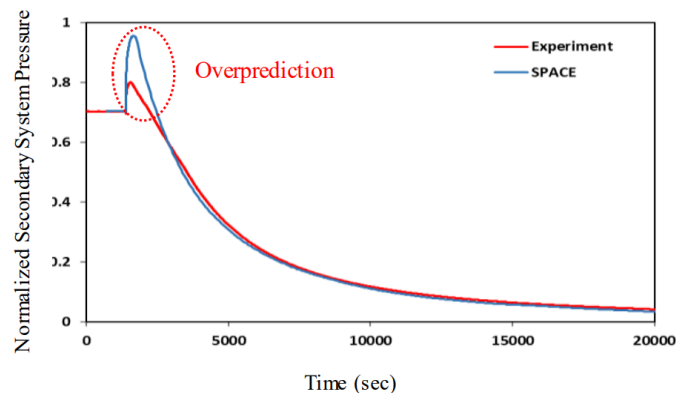


Fig. 14. Comparison of secondary system pressure

Fig. 14 shows the secondary system pressure. In the test, the SG secondary system pressure was maintained at operational pressure until the PRHRS actuation signal was operated and the MSIV and FIV were closed. The secondary system pressure increased rapidly with the actuation of the PRHRS actuation signal. Then, it decreased gradually due to the heat removal on the primary side. The SPACE code properly predicts the overall behavior of the secondary system pressure, but it slightly overpredicts the maximum secondary pressure at the beginning of the transient due to the over-prediction of the heat exchange between the primary and secondary

systems.

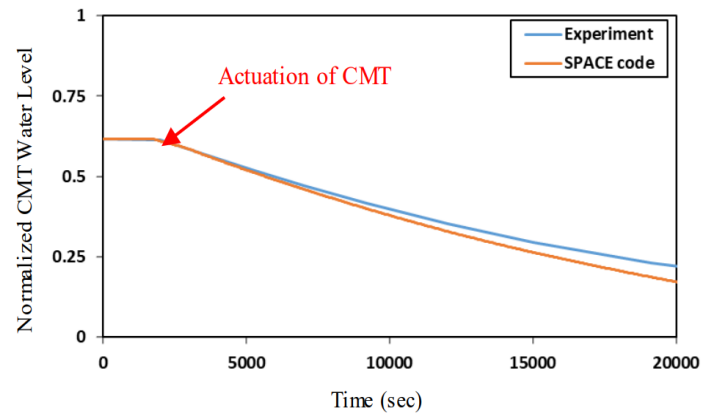


Fig. 15. CMT water level

As shown in Fig. 15, the CMT water level started at a similar time with the experiment and decreased continuously until the end of the accident. The SPACE code properly predicts the measured water level of CMT.

IV. Conclusion

Validation of the SPACE code was performed using the test results of SB-PSIS-F301 and SBPSIS-F101 at the SMART-ITL facility. The validation results showed that the overall thermalhydraulics behaviors, such as the primary system pressure, primary system temperatures, and secondary system pressure, were properly predicted for both accident scenarios. However, the SPACE code underpredicted the water level in the reactor pressure vessel because of the overprediction of the accumulated break flow. This was mainly due to the inaccuracy of the critical flow models during the two-phase flow period. Therefore, the users of the code should always take into consideration the existence of the two phases in the break node and their significant impact on the depressurization rate and the break flow rate.

Acknowledgments

This research was supported by King Abdullah City for Atomic and Renewable Energy (K.A.CARE), Kingdom of Saudi Arabia, and KAERI within the Joint Research and Development Center

References

- [1] SPACE 3.0 MANUAL VOLUME 2, S06NX08-K-1-TR-36, Rev.0, 2017.
- [2] K. K. Kim, et al., SMART: The First Licensed Advanced Integral Reactor, Journal of Energy and Power Engineering, 8, 94-102, 2014.
- [3] H. S. Park, S. J. Yi, and C. H. Song, SMR Accident Simulation in Experimental Test Loop, Nuclear

Engineering International, November 2013

- [4] Kim, Yeon-Sik, et al. "Investigation of thermal hydraulic behavior of SBLOCA tests in SMART-ITL facility." *Annals of Nuclear Energy* 113 (2018): 25-36.
- [5] Chung, Young-jong, et al. "Validation with the MARS and TASS/SMR codes based on experimental results of a pressurizer safety valve line break at the SMART-ITL facility." *Annals of Nuclear Energy* 141 (2020): 107344.

Appendix

Table V List of nomenclature used in the paper

Nomenclature	Referred to
ADS	Automatic Depressurization Systems
BMS	break measuring system
BSS	break simulating system
CMTAS	Core Makeup Tank Actuation Signal
DBA	Design Basis Accident
DEC	Design Extension Conditions
ITL	Integral Test Loop
LOCA	Loss of Coolant Accident
LOOP	Loss of Offsite Power
LPP	Low Pressurizer Pressure
NSSC	Nuclear Safety and Security Commission
PRHRS	Passive Residual Heat Removal System
PRHRAS	Passive Residual Heat Removal System Actuation Signal
PSIS	Passive Safety Injection Systems
PSV	Pressurized Safety Valve
PWR	Pressurized Water Reactor
PZR	Pressurizer
RCP	Reactor Coolant Pump
RCS	Reactor Coolant System
RPV	reactor pressure vessel
SBLOCA	Small break loss of coolant accidents
SGs	Steam Generators
SIL	Safety Injection Line
SIT	Safety Injection Tank
SITAS	Safety Injection Tank Actuation Signal
SPACE	Safety and Performance Analysis Code
TLOSHR	Total Loss of Secondary Heat Removal